

doi: 10.3788/gzxb20164507.0704001

锰钴镍型红外探测器空间环境 效应与 $1/f$ 噪声甄别方法

胡为^a, 庄奕琪^b, 包军林^b, 赵启凤^b

(西安电子科技大学 a. 机电工程学院; b. 微电子学院, 西安 710071)

摘 要: 在模拟的空间环境试验中测试了锰钴镍型红外探测器的电阻值和低频噪声参量. 采用钴-60 源分别在 10 rad(si)/s 和 0.1 rad(si)/s 的剂量率下对两组样品累积辐照到总剂量 150 krad(si), 结果表明: 在 0.1 rad(si)/s 剂量率下探测器低频噪声退化量远大于 10 rad(si)/s 剂量率下的低频噪声退化量. 对第三组样品先后施加了三种热应力, 即无偏热应力(40℃, 保持 4h), 加偏热应力(偏置电压±15 V, 40℃, 保持 600 h)和无偏热循环(-40℃到 40℃, 温度变化率 1℃/s, 峰值温度保持 1 h, 20 个循环), 结果表明: 热应力试验中, 样品电阻值变化规律相对一致, 但低频噪声的退化趋势存在明显差异, 且失效探测器表现为低频噪声突然增大. 分析表明, 无偏热应力与加偏热应力引起的低频噪声退化来源于电阻薄片内部的缺陷, 而热循环导致的低频噪声退化来源于连接 Pt 引线焊点接触处的潜在缺陷. 研究发现噪声系数是锰钴镍型红外探测器低频噪声退化的敏感参量, 热应力与热循环则可以有效甄别该类器件噪声退化.

关键词: $1/f$ 噪声; 可靠性; 伽马辐照; 热应力; 红外探测器

中图分类号: TN215

文献标识码: A

文章编号: 1004-4213(2016)07-0704001-6

Space Environment Effects and $1/f$ Noise Discrimination Method on Mn-Co-Ni Type Infrared Detectors

HU Wei^a, ZHUANG Yi-qi^b, BAO Jun-lin^b, ZHAO Qi-feng^b

(a. School of Mechano-Electronic Engineering; b. School of Microelectronics,
Xidian University, Xi'an 710071, China)

Abstract: Electrical resistance and low-frequency noise of Mn-Co-Ni type infrared detectors were measured during space-simulated environment experiments. Two groups of samples were irradiated up to 150 krad(si) accumulated dosage with a cobalt-60 source at dose rate of 10 rad(si)/s and 0.1 rad(Si)/s, respectively. The results show that $1/f$ noise increased significantly at dose rate of 0.1 rad(Si)/s, but almost unchanged at dose rate of 10 rad(Si)/s. Three thermal stresses, namely, short-term thermal burn-in without bias (40℃, hold for 4 h), extended thermal brun-in with DC bias (bias voltage of ±15 V, 40℃, hold for 600 h) and thermovacuum cycling (-40℃ to +40℃, 1℃/min, hold for 1 h, 20 cyclings), were successively applied to a third group of samples, the changes of electrical resistance of samples have similar behavior; however, the degradation of $1/f$ noise shows different trends, and all malfunctions present abrupt increment. Theoretical analysis shows that the degradations of $1/f$ noise during the short-term thermal burn-in and extended thermal burn-in with DC bias may be ascribed to the

Foundation item: The National Natural Science Foundation of China (Nos. 61076101, 61204092) and the Fundamental Research Funds for the Central Universities (No. JB150412)

First author: HU Wei(1981-), male, lecturer, M. S. degree, mainly focuses on weak signal detection technique. Email: whu@xidian.edu.cn

Supervisor(Corresponding author): ZHUANG Yi-qi (1957-), male, professor, Ph. D. degree, mainly focuses on Noise and reliability of microelectronic device application technology. Email: yqzhuang@xidian.edu.cn

Received: Dec. 16, 2015; **Accepted:** Apr. 7, 2016

<http://www.photon.ac.cn>

defects within the thermistor bulk, and the degradations of $1/f$ noise during thermal cycling may be ascribed to the defects at the contacts. These results suggest that noise figure is a sensitive parameters for describing the low-frequency noise degeneration of infrared detectors, and short-term thermal burn-in and thermal cycling are effective testing methods for discriminating $1/f$ noise of infrared detectors.

Key words: $1/f$ noise; Reliability; Gamma radiation; Thermal stress; Infrared detectors

OCIS Codes: 040.3060; 040.6808; 120.6810; 350.5610

0 Introduction

Negative Temperature Coefficient (NTC) thermistors based on solid solutions of transition metal oxides, such as Mn_3O_4 , Co_3O_4 , and NiO , have the advantages of high thermal constant (B constant) and adjustable resistivity with concentration of metal oxides. Infrared detectors manufactured from this type of NTC thermistors are widely used in various industrial and advanced applications, such as elements for temperature measurements and control, and for spacecraft attitude determination, in which area, high quality and functional reliability are required^[1-5].

The degradation of the exploitation parameters, such as electrical resistance and thermal constant B, is used to describe the stability of the thermistor. However, according to the experimental results of many samples, the escalation of their Low-Frequency Noise (LFN) is also one of the main failure modes. In 1980, NASA investigated the electrical noise in selenium-immersed thermistor bolometers at elevated temperatures. The tests showed a very rapid noise buildup on unsealed units^[4]. P. Umadevi^[5] studied the environmental durability of the infrared detectors by subjecting the detectors to different environmental tests, but these tests do not include irradiation test. Ouyang C. and Zhou W.^[2-3] use noise as a parameter to investigate the preparation method and performance of Mn-Co-Ni (MCN) type infrared detectors. These indicate that the LFN can be used to assess the quality and reliability, analyze and diagnose the defects of the device^[6]. So, a deep investigation of LFN characteristics and developing a method for discriminating $1/f$ noise of infrared detectors based on MCN thermistor are of great significance.

In this paper, we present the experimental results of the electrical resistance and LFN power spectrum density of the samples under different environmental conditions, then, the LFN characteristics of the samples under the conditions are discussed. The aim of this work is to find a more effective characterization parameter to evaluate the reliability of infrared detectors and an efficient method for discriminating $1/f$ noise of infrared detectors.

1 Experiment

High purity oxides of manganese, nickel and

cobalt in the proportion of 52 : 16 : 32 parts by weight were mixed with an organic binder. The obtained slurry was then dried in an oven. The dried powders were ground in mortar and passed through mesh sieve. The mixture powders were pressed into rectangle form in a unique groove and then sintered. Finally, thin film with dimension of $390 \mu m \times 130 \mu m$ and thickness of $10 \mu m$ were obtained. Fig. 1(a) presents the structure schematic of the MCN film. Au electrodes (thickness of $1 \mu m$) were sputtered onto two sides of the film, then, Pt wires were soldered onto each of the Au electrodes as the inner leads, with the solder joint thickness of about $50 \mu m$. The room-temperature electrical resistance of achieved thermistor is about $240 k\Omega$. Then two matched thermistors, one was used as the active element sensing the infrared radiation and the other as the compensated sensing element, were serially connected as an R-bridge circuit and immersed into Sn-As-S-Tl glass at the bottom of a Ge-window. Subsequently, as shown in Fig. 1(b). Ge-window and thermal sensors were packaged under nitrogen gas atmosphere to form the infrared detectors, so the inner space of detector was filled with nitrogen gas, which can reduce the level of thermal fluctuation noise.

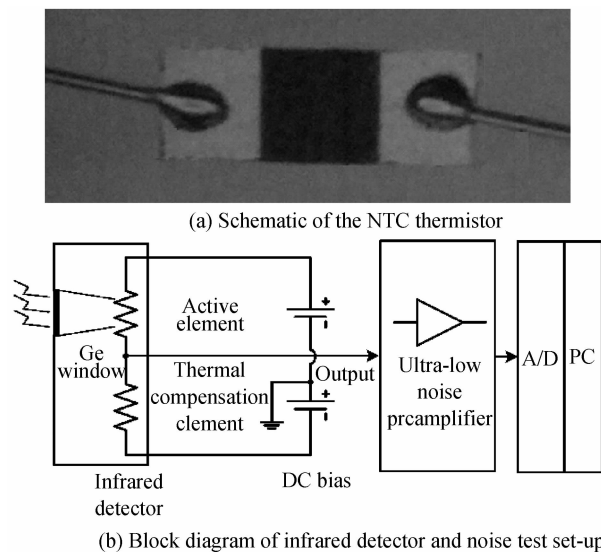


Fig. 1 Mn-Co-Ni type thermistors, infrared detector and noise test set-up

When the active element of the DC current biased detector absorbs infrared radiation, its electrical resistance decreases, result in a voltage changes in the R-bridge circuit. This voltage variation was amplified

by an ultra-low noise preamplifier and then transmitted to other processing circuit^[7]. When measuring the noise signal, the Ge-window of infrared detector was covered to avoid the influence of the infrared radiation. The amplified noise signal was captured with an A/D converter and analyzed with a PC based software. The block diagram of the noise test set-up was shown in Fig. 1(b).

Two groups of infrared detectors (RH1 ~ RH5, RL1 ~ RL5) from the same lot were irradiated using a Cobalt-60 source at room temperature to investigate the low frequency noise characteristic. The accumulated total dose is 150 krad (Si) at low dose rate of 0.1 rad (Si)/s and high dose rate of 10 rad (Si)/s, respectively. The infrared detectors were periodically removed from the radiation source to track changes in the noise as the absorbed total dose increased. The accumulated total dose test step was 10, 30, 50, 70, 100 and 150 krad (Si). Variations of electrical resistance and output noise were measured and analyzed.

Another group of samples (A1 ~ A6) under three different thermal stresses was also studied. Because the melting point of the Sn-As-S-Tl glass is about 85°C, the maximum temperature during the experimental was 40°C. Three kinds of stresses, short-term thermal burn-in (40°C, hold for 4 hours, designated as stress # 2, the condition of before applying stress designated as stress # 1), extended thermal burn-in with DC bias (bias voltage of ±15 V, 40°C, hold for 600 hours, designated as stress # 3) and thermal cycling (−40°C to +40°C, 1°C/min, hold for an hour, 20 cycling, designated as stress # 4) were sequentially applied to six samples. Electrical resistance and LFN power spectrum density were monitored before and after each of the stresses was applied.

2 Results and discussion

2.1 Degradation of electrical resistance under radiation and thermal stress

The relative variation of resistance $\Delta R/R$ is used to evaluate the degradation of the resistance. $\Delta R/R$ is defined as

$$\frac{\Delta R}{R} = \frac{R_{25\text{-poststress}} - R_{25\text{-prestress}}}{R_{25\text{-prestress}}} \quad (1)$$

where $R_{25\text{-prestress}}$ is the resistance of sample at 25°C before stress is applied, $R_{25\text{-poststress}}$ is the resistance of sample at 25°C after each stress is applied.

Fig. 2 shows the change in the DC resistance, $\Delta R/R$, as a function of applied stresses of samples. The resistance is observed to increase with applied stress. After irradiation, the increment in resistance under dose

rate of 0.1 rad(si)/s is more than that under dose rate of 10 rad(si)/s, but both no more than 4%. During thermal testing, the resistance of A4 shows the most dramatic change among the six samples, the drift is as high as 20% after stress # 4 was applied. The changes in resistance of the other five samples have the similar trends; the maximum drift is below 10% after stress # 4 was applied.

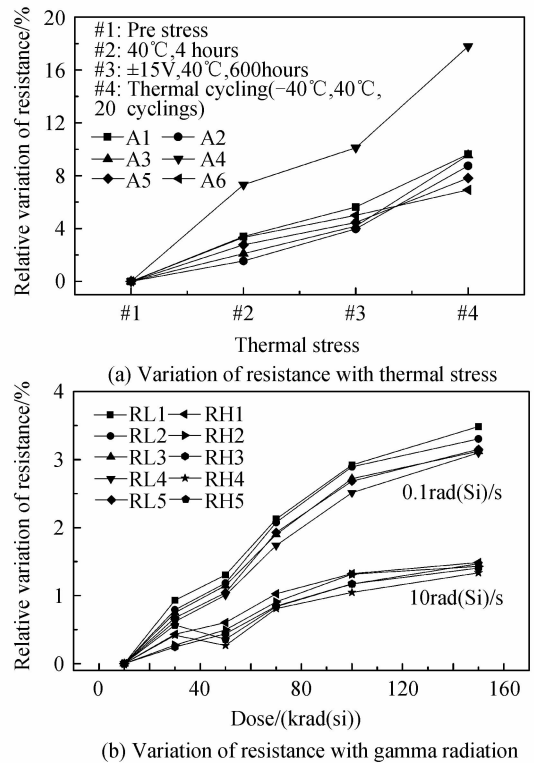


Fig. 2 Relative variation of resistance with different stresses

MCN thermistor in infrared detectors has a spinel structure, there are a lot of grains and grain boundaries in the thin film. Small polaron hopping mechanism is used to explain the conductivity. Carriers hopping in the grains and tunneling through the grain boundary barriers form a current flow in the thermistor. After gamma radiation, the density of interface defects increased, this leads to an increase in the grain boundary barrier height and then the resistivity of the thermistor.

The effect of thermal and current stress on the resistivity of the infrared detectors during test mainly arises from four sources: 1) The disproportionation of $[Mn^{3+}]/[Mn^{4+}]$ ions in the octahedral sites combined with an exchange of nickel between sublattice, results in a decrease in effective concentration of charge carriers, $Mn^{3+} Mn^{4+}$, and a consequent increase in resistivity^[8]; 2) The cationic vacancy-assisted migration of cations to their thermodynamically preferable sites under stress^[9]; 3) The thermal treatment during the metallization used to bond electrodes on ceramics may trigger the ageing

phenomenon^[10-11]; 4) The oxidation which occurs during cooling down in air after sintering may also trigger ageing^[12].

2.2 Degradation of low-frequency noise under gamma radiation

Fig. 3 shows the Power Spectrum Density (PSD) of the low-frequency noise of the sample A1 with ± 15 V DC bias voltage (total noise), without bias voltage (thermal noise) and of the ground noise of the test set-up. It can be seen that the PSD of LFN of the sample with bias has a $1/f$ dependence in the range 1 to 300 Hz, moreover, it is more than an order of magnitude higher than that of the ground noise of the test set-up.

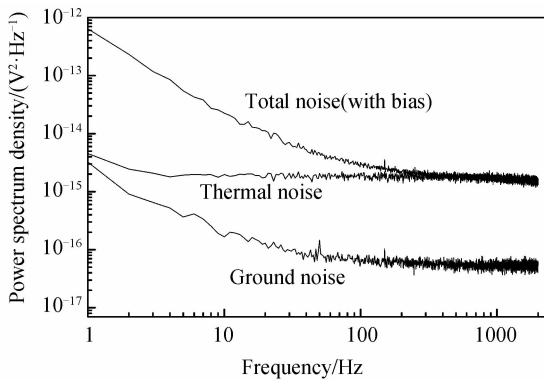
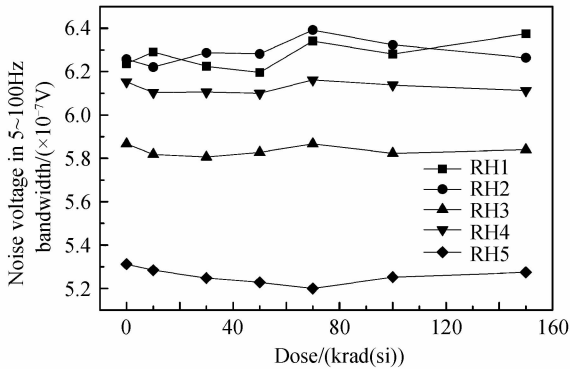
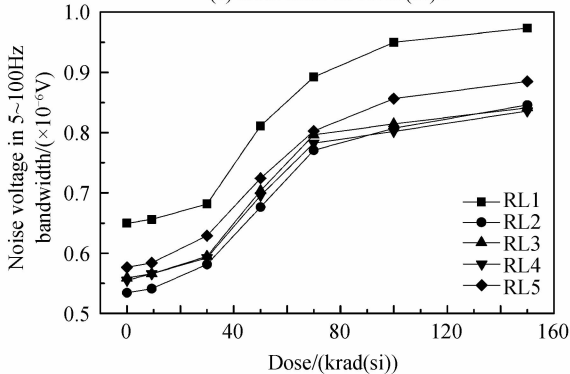


Fig. 3 The total noise, thermal noise of A1 before applying of stress and system ground noise

Fig. 4 shows the noise voltage in 5~100 Hz



(a) Dose rates of 10rad(Si)/s



(b) Dose rates of 0.1rad(Si)/s

Fig. 4 Wideband noise voltage versus absorbed total dose

bandwidth of the samples at each dose step under the dose rate of 10 rad(Si)/s (b) and 0.1 rad(Si)/s (b) respectively. It can be seen that, at high dose rate, the noise voltage of the infrared detector almost unchanged, but at lower dose rate, the noise voltage increase significantly. This indicates that the irradiation induced more defects in infrared detector at low dose rate.

2.3 Degradation of low-frequency noise under thermal stress

There are two main defects in infrared detectors, bulk defects and contacts. Defects always lead to the increase of the low frequency noise of the device. Differences on homogeneity and microstructure of the thin film may lead to discreteness on the performance of thermistor during manufacturing process. Manual bonding the inner lead to thermistor may also result in the latent defects at the electrode contact. Deep level defects in the thermistor bulk could be activated by enhanced thermal stress. Because of the different thermal expansion coefficients, defects at the electrode contact could be activated by thermal cycling test. Therefore, three thermal stress tests were designed, variations of low frequency noise during tests were used to discriminate the bulk defects and contact defects in infrared detectors.

As shown in Fig. 2, the resistance of the device increased after thermal stress, since the LFN is related to resistance, a parameter, Noise Figure (NF), is used to evaluate the reliability of infrared detectors to avoid the influence of the drift resistance. The NF is defined as the ratio of rms voltage within the bandwidth of 5 Hz to 100 Hz of the total noise to Root Mean Square (RMS) voltage within the same bandwidth of the thermal noise.

The changes of LNF as a function of applied stresses for six samples are presented in Fig. 5. According to the change trends of the NF, the samples could be divided into three classes. The first class of samples, A5, has the best quality, as its NF almost has no changes during the tests. In the second class of samples, A1 and A6, the NF has a slight variation under stress # 2 and stress # 4, but a great increase under stress # 3, indicates that the defects of these infrared detectors concentrate mainly inside the bulk of the thermistor, rather than on the electrode contact, and these defects could only be activated under tightened stress (long time ageing with bias voltage). The NF of the last class, A2, A3 and A4, has dramatic changes under all three stresses, and the changes under stress # 3 are more dramatic than that under stress # 2, which indicates that these samples have many defects both in thermistor and on the

electrode contact.

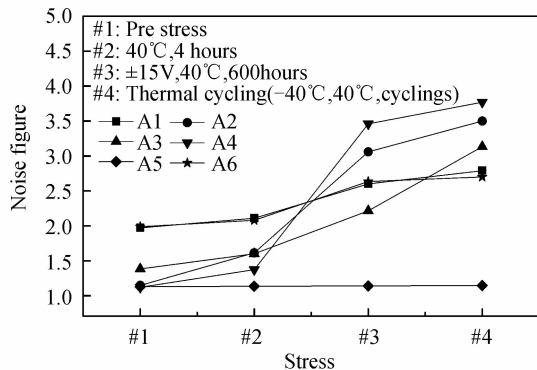


Fig. 5 Changes in NF with applied stresses

2.4 Low frequency noise mechanism and discrimination methods

According to their composition, there are two sources of low-frequency noise in the studied infrared detectors, namely, the contact noise^[13] at the solder joints which used to bound the inner Pt leads, and the thermistor bulk noise^[14]. Thermal burn-in test could result in the growth of the Intermetallic Compound (IMC) at the solder/metalization interface, and the growth rate is accelerated in the thermal cycling, moreover, the presence of grain boundaries also accelerates the growth rate^[15]. A thick IMC layer can result in degradation of the solder joint reliability and lead to the increase of the contact noise. According to the study of the LFN of thick-film resistors^[16-17], the bulk noise of the resistors comes from the conduction through conductive grains or contacts between them, and from the conduction through glass barriers due to the fluctuations caused by the presence of the traps in the glass barrier. For thermistors based on Mn-Ni-Co-O spinel ternary oxide, their conductivity is described by a thermally activated charge carriers phonon-assisted hopping between Mn^{4+} and Mn^{3+} on the octahedral sites^[18-19] and tunnelling through the grain boundaries^[20]. Thermal stress loading may accumulate defects at the grain boundaries, which affects the balance of traps at the area, then leads to the increase of the bulk noise.

According to the test results and LFN mechanism, it can be seen that: 1) The samples, which have an increase in NF after applied stress #2 (40°C, hold for 4 h), all have more increases in NF after applied stress #3 (bias voltage of ± 15 V, 40°C, hold for 600 h). There is a positive correlation between them. This gives a fast way of discriminating LFN of NTC infrared detectors. That is, using of the amount of LFN degradation during the short-term isothermal ageing to evaluate the amount of LFN degradation during the long-term, DC voltage biased isothermal ageing, thus, shortens the test time. 2) Applying of stress #4

(-40°C to +40°C, 1°C/min, hold for 1 h, 20 cyclings) is a effective way to evaluate the contact noise at the solder joints which used to bound the inner Pt leads of infrared detectors based on Mn-Ni-Co-O spinel ternary oxide.

3 Conclusion

The degradation of LFN is one of the main failure modes of Mn-Ni-Co type infrared detectors. Applying of several kinds of stresses were used to characterize the degradation of the samples. The low-frequency noise of infrared detectors based on Mn-Ni-Co-O spinel ternary oxide comes from the contact at the solder joints which used to bound the inner Pt leads and the bulk of the thermistors. The LFN characteristic degenerated under a dose rate of 0.1rad(si)/s gamma radiation. During thermal tests, electrical resistance of the samples with the same chemical composition and technological parameters almost have the similar behaviors, while the degradations of LFN show different trends. Noise figure is a more effective parameter to evaluate the reliability of the infrared detectors. Short-term thermal burn-in and thermal cycling are the efficient methods for discriminating 1/f noise of NTC infrared detectors based on Mn-Ni-Co-O spinel ternary oxide.

References

- [1] KARANTH S, SUMESH M A, SHOBHA V, *et al.* Infrared detectors based on thin film thermistor of ternary Mn-Ni-Co-O on micro-machined thermal isolation structure[J]. *Sensors and Actuators A: Physical*, 2009, **153**(1): 69-75.
- [2] OUYANG Cheng, ZHOU Wei, WU Jing, *et al.* Uncooled bolometer based on $Mn_{1.56}Co_{0.96}Ni_{0.48}O_4$ thin films for infrared detection and thermal imaging[J]. *Applied Physics Letters*, 2014, **105**(2): 022105.
- [3] ZHOU Wei, OUYANG Cheng, WU Jing, *et al.* Investigation on preparation method and performance of $Mn_{1.56}Co_{0.96-x}Ni_{0.48}Cu_xO_4$ thin film IR detector[J]. *Infrared and Laser Engineering*, 2014, **43**(4):1073-1079.
- [4] TARPLEY J L, SARMIENTO P D. Investigation of electrical noise in selenium-immersed thermistor bolometers[J]. *NASA STI/Recon Technical Report N*, 1980, **80**: 31778.
- [5] UMADEVI P, NAGENDRA C L. Preparation and characterisation of transition metal oxide micro-thermistors and their application to immersed thermistor bolometer infrared detectors[J]. *Sensors and Actuators A: Physical*, 2002, **96**(2-3): 114-124.
- [6] BAO Jun-lin, ZHUANG Yi-qi, DU Lei, *et al.* Investigation of mechanisms on 1/f noise and G-R noise in optoelectronic coupled devices[J]. *Acta Photonica Sinica*, 2005, **34**(6): 857-860.
- [7] HE Xiao-mu, LI Zi-tian. The infrared detector photoelectricity performance measure system [J]. *Acta Photonica Sinica*, 2000, **29**(4): 376-379.
- [8] CASTELAN P, AI B, LOUBIERE A, *et al.* Aging study of nickel-copper-manganite negative temperature coefficient thermistors by thermopower measurements[J]. *Journal of Applied Physics*, 1992, **72**(10): 4705.
- [9] FANG Dao-lai, ZHENG Cui-hong, CHEN Chu-sheng, *et al.*

- Aging of nickel manganite NTC ceramics [J]. *Journal of Electroceramics*, 2008, **22**(4): 421-427.
- [10] METZ R. Electrical properties of N. T. C. thermistors made of manganite ceramics of general spinel structure: $Mn_{3-x-x'}M_xN_{x'}O_4$ ($0 \leq x + x' \leq 1$; M and N being Ni, Co or Cu). Aging phenomenon study [J]. *Journal of Materials Science*, 2000, **35**(18): 4705-4711.
- [11] FRITSCH S, SARRIAS J, BRIEU M, *et al.* Correlation between the structure, the microstructure and the electrical properties of nickel manganite negative temperature coefficient (NTC) thermistors [J]. *Solid State Ionics*, 1998, **109**(3): 229-237.
- [12] GROEN W A, METZMACHER C, HUPPERTZ P, *et al.* Aging of NTC ceramics in the system Mn-Ni-Fe-O [J]. *Journal of Electroceramics*, 2001, **7**(2): 77-87.
- [13] KOLAHDOUZ M, AFSHAR FARNIYA A, ÖSTLING M, *et al.* Improving the performance of SiGe-Based IR detectors [J]. *ECS Transactions*, 2010, **33**(6): 221-225.
- [14] LEE M, YOO M. Detectivity of thin-film NTC thermal sensors [J]. *Sensors and Actuators A: Physical*, 2002, **96**(2): 97-104.
- [15] XU Lu-hua, PANG J H L, PRAKASH K H, *et al.* Isothermal and thermal cycling aging on IMC growth rate in lead-free and lead-based solder interface [J]. *Components and Packaging Technologies, IEEE Transactions on*, 2005, **28**(3): 408-414.
- [16] KOLEK A, STADLER A W, PTAK P, *et al.* Low-frequency 1/f noise of RuO₂-glass thick resistive films [J]. *Journal of Applied Physics*, 2007, **102**(10): 103718-9.
- [17] MRAK I, JEVTIC M M, STANIMIROVIC Z. Low-frequency noise in thick-film structures caused by traps in glass barriers [J]. *Microelectronics Reliability*, 1998, **38**(10): 1569-1576.
- [18] PETRIC A, LING H. Electrical conductivity and thermal expansion of spinels at elevated temperatures [J]. *Journal of the American Ceramic Society*, 2007, **90**(5): 1515-1520.
- [19] SCHMIDT R, BASU A, BRINKMAN A W. Small polaron hopping in spinel manganates [J]. *Physical Review B*, 2005, **72**(11): 115101.
- [20] PARK K. Improvement in electrical stability by addition of SiO₂ in (Mn_{1.2} Ni_{0.78} Co_{0.87-x} Cu_{0.15} Si_x) O₄ negative temperature coefficient thermistors [J]. *Scripta Materialia*, 2004, **50**(4): 551-554.